

## COGNITIVE NEUROSCIENCE

# Inactivation of lateral connections in cat area 17

Cyrille C. Girardin\* and Kevan A. C. Martin

Institute of Neuroinformatics, ETH/University of Zurich, Zurich, Switzerland

**Keywords:** GABA, orientation selectivity, visual system

## Abstract

Excitatory synapses arising from local neurons in the cat visual cortex are much more numerous than the thalamocortical synapses, which provide the primary sensory input. Many of these local circuit synapses are involved in the connections between cortical layers, but lateral connections within layers provide a major component of the local circuit synapses. We tested the influence of these lateral connections in the primary visual cortex of cats by inactivating small patches of cortex about 450  $\mu\text{m}$  lateral from the recording pipette. By use of the neurotransmitter  $\gamma$ -aminobutyric acid (GABA), small patches of cortex were inhibited and released from inhibition in seconds. Orientation tuning curves derived from responses to oriented drifting gratings were obtained during short control periods interleaved with periods of GABA inactivation. About 30% of the cells (18/62, recorded in all layers) changed their orientation tuning when a small portion of their lateral input was silenced. There was no broadening of the orientation tuning curve during lateral inactivation. Instead, the recorded cells shifted their preferred orientation towards the orientation of the inactivated site. One explanation is that the GABA inactivation alters the balance of excitatory and inhibitory inputs to a cell, which results in a shift of the cell's preferred orientation.

## Introduction

Neurons of the primary visual cortex (V1 or area 17) have properties such as orientation preference, direction selectivity, and contrast adaptation, which are weak or absent in the visual thalamus. Although these emergent properties are thought to be largely due to the pattern of feedforward thalamic projections (Hubel & Wiesel, 1962; Reid & Alonso, 1995; Ferster & Miller, 2000), detailed anatomical studies have revealed that only 5% of all excitatory synapses in layer 4 originate from thalamic relay cells (Winfield & Powell, 1983; LeVay, 1986; Ahmed *et al.*, 1994; Binzegger *et al.*, 2004). Most cortical synapses arise from local neurons whose axons also form extensive lateral projections (Martin & Whitteridge, 1984; Gilbert & Wiesel, 1989; Binzegger *et al.*, 2004).

Eysel *et al.* inactivated the lateral connections in the cat visual cortex using  $\gamma$ -aminobutyric acid (GABA). They found that the orientation tuning width of superficial layer cells increased (Eysel *et al.*, 1990; Crook *et al.*, 1991, 1997; Crook & Eysel, 1992). They interpreted this as evidence that the orientation selectivity of cortical neurons was sharpened by cross-orientation inhibition, and thus that the GABA application had mainly blocked the action of the large basket cells (Morrone *et al.*, 1982; Crook & Eysel, 1992). Although a 'Mexican hat' profile of central excitation and lateral inhibition is

widely used in modelling to prevent runaway excitation, it is clear that the major lateral connections in the cat V1 are excitatory and extend further than the lateral inhibitory projections in all layers (Martin *et al.*, 1983; Martin & Whitteridge, 1984; Kisvárdy *et al.*, 1985) [see discussion in Martin (2002)].

Experiments using adaptation paradigms (Müller *et al.*, 1999; Dragoi *et al.*, 2000, 2001; Felsen *et al.*, 2002) have confirmed that the cortical circuitry actively participates in generating orientation selectivity. Moreover, these results suggest that orientation plasticity is present in V1. Similar mechanisms might be involved in perceptual learning, as training paradigms can change the shape of the orientation tuning curves of individual neurons in V1 (Schoups *et al.*, 2001). Our hypothesis is that the lateral architecture has a significant role to play in this plasticity.

In cat area 17, the lateral patches formed by groups of superficial pyramidal cells are about 300–500  $\mu\text{m}$  in size, with a pattern that connects like-to-like in the overall orientation map (Gilbert & Wiesel, 1989; Callaway & Katz, 1990, 1991; Luhmann *et al.*, 1990; Kisvárdy & Eysel, 1992; Lübke & Albus, 1992; Kisvárdy *et al.*, 1997; Schmidt *et al.*, 1997; Buzás *et al.*, 2006). Short-range connections (< 0.5 mm) seem to be less specific, but are also dominated by like-to-like connections, by virtue of the fact that their neighbouring neurons have similar orientation preferences (Kisvárdy *et al.*, 1997; Yousef *et al.*, 1999, 2001; Mariño *et al.*, 2005; Buzás *et al.*, 2006). Despite numerous studies, our understanding of the functional role of lateral connections remains incomplete. Here, we tested the hypothesis that the shape of the orientation tuning curve of single neurons depends on the lateral cortical connections.

Correspondence: Dr C. Girardin, \*Present address below.  
E-mail: cyrille.girardin@uni-konstanz.de

\*Present address: Universität Konstanz, Biologie – Neurobiologie, Universitätstrasse 11 (M11), 78457 Konstanz, Germany

Received 2 September 2008, revised 23 February 2009, accepted 13 March 2009

## Materials and methods

### Animal preparation

Twelve adult cats were used for this study. The experimental protocols for these experiments were approved by the Canton of Zurich Veterinary Office, which issued the licence No. 50/3002 for the project "Microcircuits of neocortex" to K.A.C.M. For a detailed description of the surgical procedure and animal maintenance, see Girardin *et al.* (2002). Briefly, anaesthesia was induced with a mixture of xylazine (0.5 mg/kg; Rompun; Bayer, Leverkusen, Germany) and ketamine (10 mg/kg, Narketan; Chassot, Bern, Switzerland), and maintained with Saffan (alphadolone + alphaxolone; Schering-Plough Animal Health, Welwyn Garden City, UK). Saffan (~0.1–0.2 mL/kg/h) was given through a venous cannula. Animals were paralysed [mixture of gallamine triethiodide (5 mg/kg/h) and d-tubocurarine chloride (0.5 mg/kg/h)], and ventilated with a 30 : 70 mixture of O<sub>2</sub>/N<sub>2</sub>O through a tracheal cannula. Halothane was used for surgical procedures (e.g. cannulations and craniotomy, 1–2%). Electroencephalogram, electrocardiogram, blood pressure, rectal temperature and expired CO<sub>2</sub> were monitored continuously, and kept in physiological ranges. Neutral power lenses and atropine were applied on the eyes. Eyes were refracted and focused at a distance of 57 cm.

### Recording and iontophoresis

Glass pipettes (tip broken to 2–4  $\mu$ m diameter) filled with a recording solution and 1.5% biocytin (Sigma) were used to record single cells in layer 2–6 of V1. The preferred orientation was determined, and the receptive field was plotted manually on a tangent screen. Biocytin was injected with +2 to +4  $\mu$ A for 1–2 min to identify the recording site.

GABA (Fluka, 0.5 M, pH 3.5) was iontophored using multibarrel pipettes. One or more barrels were used for injection, and the total current was typically +100 to +120 nA. The inactivation periods lasted 2 or 3 min, and were interleaved with control recording periods, during which a retention current (–5 to –10 nA) was applied. Another barrel was used to record the multiunit activity at the inactivation site. One barrel filled with NaCl was used for current balance. In three cats, the recording at the inactivation site was performed using a single-barrel pipette (tip size about 2–4  $\mu$ m) glued to the inactivation pipette (horizontal distance, 0–30  $\mu$ m). Pontamine sky blue (Sigma) was iontophored at the end of the recording at the inactivation site to identify the inactivated location. The recording and inactivation pipettes were placed on the cortical surface and advanced into the cortex with two independent microdrives. The depth of both pipettes was kept approximately similar, to achieve lateral inactivation. To bring both pipette tips close enough, the recording pipette holder was tilted at an angle of 10–15°. The cortex was stabilized with a plastic chamber filled with agar. In eight cats, optical imaging of intrinsic signal was performed before recording and inactivation. Single and orientation colour-rendered maps were obtained in six cats. These maps were only used to target the pipette penetrations, and were not further analysed. The orientation selectivity at the inactivation and recording sites was determined electrophysiologically.

### Visual stimulation and data acquisition

Drifting sine wave gratings were presented to all cells. Temporal (range, 0.5–4 Hz; mean, 1.3 Hz) and spatial (range, 0.4–2.5, mean, 0.9 cycle/degree) frequencies were optimized for each cell. The number of cycles ranged from four to 12, and was adjusted according to the temporal frequency to keep the stimulation time short (range,

2.8–8 s; mean, 4.8 s) so as to avoid contrast adaptation [see, for example, Ohzawa *et al.* (1985)]. The gratings (10° × 10°) were displayed on a screen (Tektronix 608 monitor, phosphor P31; USA) placed at a distance of 57 cm from the eyes. The receptive field was centred on the screen. The grating contrast was typically 30–50%, and was below the cell's saturation level. The stimulus orientation varied in a pseudo-random order from –180° to +180° around the preferred orientation. To detect small changes in the tuning curve, small orientation steps (range, 4–13.8°; mean, 9.2°) were used. For sharply tuned cells, the range of tested orientations was narrower (e.g. –60° to +60°). A blank screen was shown for about 1 s between the stimuli. The stimulus was controlled by the vs software [Cambridge Electronic Design (CED), Cambridge, UK]. Data acquisition was performed using a CED 1401 A/D converter connected to the software SPIKE2 (CED). Multiunit activity was recorded at the inactivation site. Spikes recorded from the target neuron were isolated using an electronic spike trigger (Digitimer, Welwyn Garden City, UK), and the spike times were stored in a computer.

The receptive field of the recorded cell was first plotted manually. When possible, the receptive field and optimal orientation of the multiunit activity ('hash') and, occasionally, of single cells at the inactivation site were also plotted. The average difference between the preferred orientation determined by hand-plotting and the tuning curve measured with a computer was about 5° (i.e. less than the interval between successive computer-controlled stimulus orientations, data not shown). This means that the preferred orientation determined manually was accurate and was thus used to compare the preferred orientation at the inactivation and recorded sites (Fig. 10).

### Data analysis

Cells were 'simple' if they had spatially separate ON and OFF regions, and 'complex' if the ON and OFF subfields overlapped. Orientation tuning curves were plotted for control and GABA inactivation conditions. Control tuning curves consisted of trials recorded before the iontophoresis started (5 min) and trials recorded after termination of each period of iontophoresis. Usually, some trials (1–1.5 min) just after GABA iontophoresis termination were not included, so as to ensure complete recovery. GABA tuning curves consisted of trials recorded during GABA injection. Trials recorded from several injection periods were combined. As each cycle of a grating produced a reliable response in cortical cells, each grating cycle was considered as a single trial. Note that this did not change the mean response to each orientation calculated in spikes per second, but allowed for a more robust statistical analysis. All results are presented without subtraction of the spontaneous activity. Adaptation during stimulation was tested by comparing the mean response amplitude to the first and last grating cycles at the preferred orientation (two-sample *t*-test, two-tailed, *P* < 0.05; see Fig. 2D). The stimulus presentations and the iontophoresis periods were not synchronized, so the number of trials varied. The mean number of trials (i.e. grating cycles) per orientation was 23 (range, 4–72 grating cycles). The preferred orientation was defined as the maximum of the orientation tuning curve. To assess the effect of GABA on the orientation tuning curve, the mean response to each orientation under control conditions was compared with the mean response obtained during GABA ejection. A change in preferred orientation was significant if the control and GABA tuning curves peaked at different orientations, and if the mean response at one of the peaks under one condition (either control or GABA) was significantly different (two-sample *t*-test, two-tailed, *P* < 0.05) from the response under the alternative condition for the same stimulus orientation.

According to these criteria, each cell was scored as having a significant GABA effect on its preferred orientation or having no significant effect. In two cells, both tuning curves peaked at the same location, but as the response decreased significantly on one side of the peak and significantly increased on the other side, these cells were also considered as having a significant effect.

An orientation index (OI) was calculated with the following equation (Sato *et al.*, 1996):

$$OI = \frac{\sqrt{[\sum (R_i \times \sin(2 \times O_i))]^2 + [\sum (R_i \times \cos(2 \times O_i))]^2}}{\sum R_i}$$

$R_i$  represents the mean response magnitude to each orientation  $O_i$ . When a smaller range of orientations than  $-180^\circ$  to  $180^\circ$  was tested around the preferred orientation (e.g.  $-60^\circ$  to  $60^\circ$ ), the response magnitude outside the tested range was assumed to be zero. If the index is close to one, the cell is very selective, whereas an index close to 0 means that the cell responded to all orientations with the same amplitude. For the calculation of the preferred orientation using Gaussian fit and the vector averaging method (see Figs 8 and 9B), only the mean responses  $\pm 60^\circ$  around the measured peak were used. This improved the quality of the fit.

### Histological analysis

At the end of the experiment, the animal was deeply anaesthetized with a Saffron solution (3–5 mL, 1:1 dilution with saline) until the electroencephalogram became flat, and then perfused intracardially with normal saline followed by 4% paraformaldehyde, 0.3% glutaraldehyde, and 15% picric acid in 0.1 M phosphate buffer. Blocks of the fixed brain were serially sectioned (80  $\mu\text{m}$ ) in the transverse plane to identify the recorded and inactivated sites. Biocytin injections were revealed with an enzymatic reaction using the ABC kit (Vector Laboratories, Burlingame, USA). The pontamine injection sites were visible without further processing.

### Results

The results are based on 62 recording/inactivation pairs for which an orientation tuning curve could be recorded under control conditions and under conditions where a small patch of cortex lateral to the recording site was inactivated by GABA iontophoresis. An interleaved protocol was used in which responses to drifting oriented gratings were recorded during short control (5 min) and GABA inactivation (2–3 min) periods. The main effect of inactivation was a change in the peak location of the tuning curve when the recording and inactivated pipettes were located in the same layer. The effect was observed across the entire cortical depth (layer 2–6). The cells showing a change in peak location did not show a broadening in tuning.

Figure 1 illustrates two examples of recordings at the inactivation site during the interleaved protocol. The responses (single unit, Fig. 1A; multiunit, Fig. 1B) to visual stimulation were inhibited during GABA iontophoresis (duration of 180 s, upper deflection of the trace in Fig. 1C). Note that the responses recovered immediately after termination of the iontophoresis.

### Spontaneous activity and adaptation

In every case, we performed a control to check that the recorded cells were not directly inactivated by GABA. As GABA could have

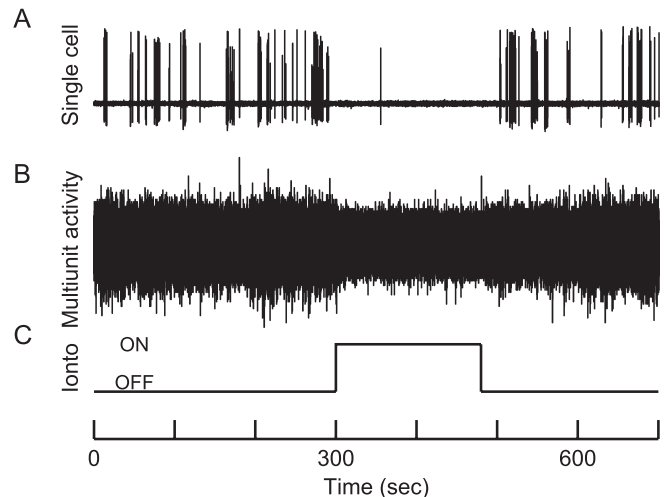


FIG. 1. Examples of recordings at the inactivation site indicating the effectiveness and the rapidity of the  $\gamma$ -aminobutyric acid (GABA) inhibitory effect. (A) Single cell recorded from a pipette glued to the inactivation pipette. (B) Multiunit activity recorded in another experiment from the recording barrel of a multibarrel inactivation pipette. (C) Inactivation protocol. Recording started with 5 min of control, and GABA iontophoresis and control recordings were then interleaved. Only one inactivation period is shown here, for clarity, but generally several were used. Note that the single cell in A and the multiunit in B were inactivated during GABA iontophoresis (upper deflection from 300 to 480 s). The cells recovered immediately after the termination of the inactivation. The recordings in both A and B were performed during visual stimulation with oriented gratings.

affected the general excitability of the cells by directly inhibiting the cell being recorded, we checked whether the spontaneous activity was inhibited. We examined both single-cell activity (Fig. 2A and B) and population activity (Fig. 2C). We found only one cell in which there was a significant GABA effect on the orientation tuning curve and the spontaneous activity changed significantly (cells were tested using a two-sample *t*-test, two-tailed,  $P < 0.01$ ). The change in spontaneous activity was very small (0.32 spikes/s, black square in Fig. 2B), and it was an increase rather than a decrease, indicating that the cell itself was not directly inhibited by the GABA. As a direct effect of GABA on this cell can be ruled out, this cell was included in the further analyses. The spontaneous activity changed significantly in two cells that showed no significant GABA effect on their tuning curve (black dots in Fig. 2B). Note that most cells had a low spontaneous activity (Fig. 2B), as is generally the case for cortical cells. At the population level, the mean spontaneous activity for all cells was unchanged during control and GABA application (two-sample *t*-test, two-tailed,  $t_{60} = 0.099$ ,  $P = 0.92$ ), and was also not different between the groups that had no GABA effect and those that had a GABA effect during GABA injection (Fig. 2C, two-sample *t*-test, two-tailed,  $t_{60} = 0.03$ ,  $P = 0.98$ ). Therefore, we can discount the possibility that the changes in orientation tuning were due to direct effects of GABA inhibition of the recorded neuron.

We then analysed adaptation during the stimulus presentation. We specifically checked that the drifting grating did not produce adaptation because it could change the preferred orientation (Dragoi *et al.*, 2000). Here, adaptation would occur if the response amplitude to the last grating cycle was smaller than the response to the first cycle (see Materials and methods). This comparison was performed for each cell for the control and GABA conditions (Fig. 2D). Some degree of adaptation was observed in only 8/62 cells (five cells, denoted '1' in Fig. 2D, with adaptation either during control or GABA application, and three cells, denoted '2' in Fig. 2D, with adaptation during both

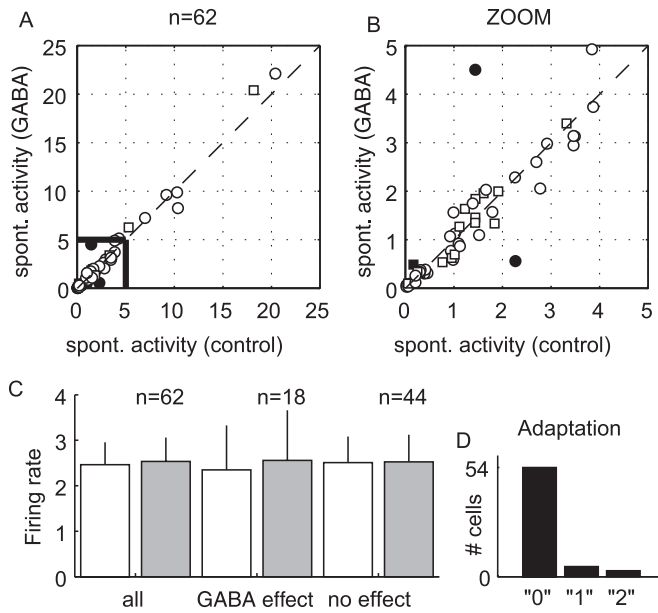


FIG. 2. Spontaneous activity measured during the interstimulus intervals and adaptation during stimulus presentation. (A) On the scatter plot, the spontaneous activity during  $\gamma$ -aminobutyric acid (GABA) injection is plotted against the spontaneous activity during control application. Axis units are spikes/s. Open symbols represent cells with no significant change in spontaneous activity between control and GABA. Closed symbols are for cells showing a significant increase (two cells) or decrease (one cell) in spontaneous activity during remote GABA iontophoresis (two-sample *t*-test, two-tailed,  $P < 0.01$ ). Circles represent cells with no significant GABA effect, and squares cells with a significant GABA effect (18 cells), according to criteria described in Materials and methods. (B) Enlarged view of the data points contained within the box in A. Note that only one cell having a significant GABA effect (black square) also has a significant change in its spontaneous activity (see text for details). (C) Comparison of control and GABA conditions for the population. Left, all cells ( $n = 62$ ) pooled. Middle, only cells with a significant GABA effect ( $n = 18$ ). Right, cells with no significant GABA effect ( $n = 44$ ). White bars, control; grey bars, GABA. The bar height is the mean response, and error bars are standard errors of the mean; *y*-axis units are spikes/s. (D) Bars show the number of cells that did not adapt ("0",  $n = 54$ ), adapted in one condition (either control or GABA, "1",  $n = 5$ ) or adapted in both conditions (control and GABA, "2",  $n = 3$ ) during the stimulus presentation (see text for details).

control and GABA application). None of the eight cells that showed some adaptation changed their preferred orientation. Thus, the adaptation mechanism described in Dragoi *et al.* (2000), which modifies the preferred orientation, cannot explain the effects on the orientation tuning curve reported below.

#### Effect of GABA on orientation tuning

Two orientation tuning curves were plotted for every cell recorded, one curve for the control response, and one for the response during remote GABA inactivation. Simple and complex cells were pooled together, as no differences in behaviour were found between the two physiological cell types. The criteria for a significant effect, described in Materials and methods, were chosen because they allowed small changes to be detected in the tuning curves of control and GABA conditions. Indeed, it was possible to detect effects in response amplitude for a single orientation. Moreover, these criteria do not make any assumptions about the shape of the orientation tuning curve.

Two examples are shown in Fig. 3. In both cases, the preferred orientation change was due to an asymmetrical increase in the response around the peak. For the cell presented in Fig. 3, A1, the

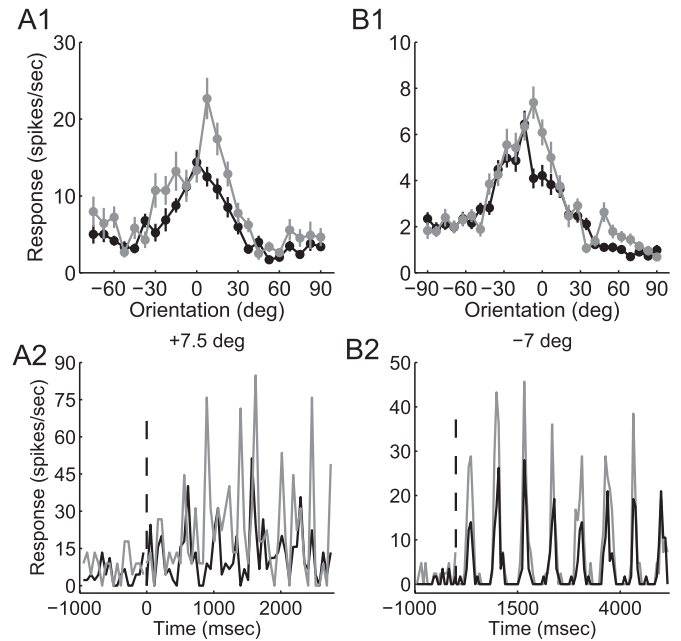


FIG. 3. Examples of the effect produced by  $\gamma$ -aminobutyric acid (GABA). (A1) The effect was an asymmetrical response increase leading to a peak shift. The *x*-axis is the stimulus orientation, and the *y*-axis is the cell response in spikes/s. The black tuning curve was recorded under control conditions, and the grey curve under GABA conditions. Error bars are standard errors of the mean. The recording (complex cell) and the inactivation were in layer 5. (A2) The PSTH shows the response to each cycle of the grating (four cycles) at the peak of the GABA orientation tuning curve ( $+7.5^\circ$ ) for control (black) and GABA (grey) conditions. The grating was presented for 2800 ms at time 0 (vertical dashed line). The bin size is 56 ms. (B1) Another example of asymmetrical response increase leading to peak shift. The neuron (simple cell) was recorded in layer 5, and the inactivation was in layer 4. (B2) Corresponding PSTH for orientation  $-7^\circ$  (peak of the GABA tuning curve; colours as in A; eight cycle grating presented for 5200 ms). The bin size is 52 ms.

recording and the inactivation pipettes were in layer 5 (histology shown in Fig. 5). During inactivation, the peak response shifted by  $8^\circ$ . Surprisingly, during GABA iontophoresis, the peak response increased by 63% (from 14.3 spikes/s at  $0^\circ$  to 22.7 spikes/s at  $7.5^\circ$ ). The response increase is also evident in the histograms in Fig. 3, A2, where the responses to a drifting grating oriented at  $7.5^\circ$  during control recordings (black) and GABA iontophoresis (grey) are superimposed. A similar case is shown in Fig. 3, B1. The recording was from layer 5, whereas the inactivation was in layer 4. The peak response shifted by  $7^\circ$ , and Fig. 3, B2 shows the amplitude increase at  $-7^\circ$  relative to control.

The effect of GABA varied from cell to cell. When effects were seen, the response to one or more orientations around the optimal orientation decreased or increased during GABA inactivation. Increases on one side and decreases on the other side of the peak resulted in a shift of the tuning curve. This shift is illustrated in Fig. 4A. A common effect was a decrease in activity at the peak and a small increase at an orientation close to the peak, as shown in Fig. 4B and C. In those cells, only one point close to the peak was significantly reduced during GABA application. Nevertheless, this also produced a shift of the preferred orientation of the cell. For the neuron presented in Fig. 4C, the response at the peak decreased dramatically and another peak appeared, so shifting the preferred orientation of the cell. Effects on the preferred orientation, as illustrated in Fig. 4, were observed in 18/62 cells. Out of 62 pairs, 34 were recorded from cats where optical maps were used to place both recording and inactivation

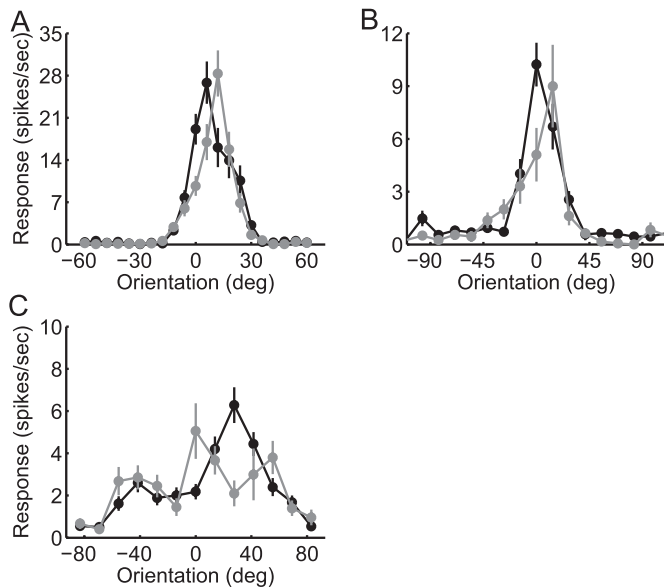


FIG. 4. Examples of  $\gamma$ -aminobutyric acid (GABA) effect on the orientation tuning curves. No broadening occurred here. Symbols and colours as in Fig. 3. The neuron (complex cell) presented in A showed a shift of the entire tuning curve, whereas the effect on the cells presented in B and C (simple cells) was a decrease in response at the peak. The recording and inactivation locations were not always recovered histologically for those cells.

pipettes within similar orientation columns. With this method, we found a significant effect in 11/18 pairs, whereas the other seven pairs with significant GABA effects were found in cats in which optical maps were not used to target the penetrations.

#### Anatomical relationship between recording and inactivation sites

Figure 5 illustrates one penetration in which three cells were recorded and four inactivation sites were tested. Two inactivation/recording pairs from this penetration are shown. Cell C1 was located in layer 4, and the tip of the GABA pipette was in the upper part of layer 5 (IN1). In this relationship, the tuning curve did not shift. Both pipettes were then advanced. The inactivation pipette remained in layer 5 (IN2), but the recording pipette passed from layer 4 to layer 5 (C2). In this relationship, a large effect was observed (this is the same cell shown in Fig. 3A). The horizontal distance between C2 and IN2 was about  $220 \mu\text{m}$ . Even at this short distance, GABA did not affect the recorded cell directly, as indicated by no change in the spontaneous activity and an increase in the cell's response during GABA inactivation. The first cell encountered in this penetration (see white star in Fig. 5) was recorded in layer 3, whereas the inactivation was also in that layer. In this case, GABA produced a modest effect on the tuning curve (data not shown).

Figure 6 shows a cell in layer 2/3 that changed its preferred orientation during the remote inactivation with GABA in the same layer (Fig. 6A). Biocytin, injected at the recording site, retrogradely labelled a pyramidal cell in the vicinity of the inactivation site (arrow in Fig. 6C). This shows the existence of monosynaptic anatomical connections between the inactivated and the recorded sites. The presence of an axon running from the inactivation site to the recorded site is shown in the partial reconstruction in Fig. 6B.

Of 18 pairs with a significant GABA effect, it was possible to identify histologically both the inactivation and the recording location

in seven cases (Fig. 7A). For the analysis, the inactivation sites were aligned and the horizontal distance to the recording site was measured. The inactivation and the recording sites were not in the same layer in only one case. In all other cases (6/7, one cell on the layer border), the significant GABA effect occurred only when the recording and the inactivation sites were within the same layer. The histological analysis for cells with no GABA effect is shown in Fig. 7B ( $n = 11$ ). In general, we found that the recording and inactivation sites were in different layers when GABA had no effect (8/11 cases in different layers, two cases in the same layer, and one case with inactivation on the layer border). The mean horizontal distance between the pipettes was  $383 \pm 73 \mu\text{m}$  (mean  $\pm$  standard error of the mean), and was not significantly different from the mean distance ( $451 \pm 75 \mu\text{m}$ ) found between pipettes when there was a GABA effect (two-sample *t*-test, two-tailed,  $t_{16} = 0.62$ ,  $P = 0.54$ ).

#### Validation of the shift criteria

To make a group comparison of the cells showing a GABA effect and those that did not, we fitted the orientation tuning curves with a Gaussian (see Materials and methods). For cells with no significant GABA effect, the mean peak difference in the Gaussian fits between control and GABA was  $1.6^\circ \pm 0.2^\circ$  (mean  $\pm$  standard error of the mean), and for cells with a significant GABA effect, the difference was  $4.5^\circ \pm 1.2^\circ$ . This difference in mean peak shift was significant (two-sample *t*-test, one-tailed,  $t_{60} = 3.5$ ,  $P = 0.000433$ ; Fig. 8, left). The same analysis on the two populations of cells was performed using the vector averaging method (Swindale, 1998; Dragoi *et al.*, 2000) to calculate the preferred orientation, and it yielded similar conclusions. The mean shift for the group showing no GABA effect was  $1.4^\circ \pm 0.2^\circ$ , and it was  $2.7^\circ \pm 0.7^\circ$  for cells showing a GABA effect. This difference was significant (two-sample *t*-test, one-tailed,  $t_{60} = 2.3$ ,  $P = 0.0137$ ; Fig. 8, right).

Both methods show that the criteria used in the present study were sensitive enough to detect a small shift of the preferred orientation. Note that the difference in the no GABA effect group was larger than zero because the absolute peak difference was used. The difference between the peaks in the group with a GABA effect was the result of an actual shift, whereas the difference that occurred in the group with no GABA effect was due to small fluctuations in the cells' responses.

#### Tuning width and response amplitude

Unlike in previous studies (Eysel *et al.*, 1990; Crook *et al.*, 1991, 1997; Crook & Eysel, 1992), the GABA inactivation that we used did not cause the tuning curve to broaden. Some possible explanations for the difference between our study and those of Eysel *et al.* are discussed below. The OI for GABA and control conditions is plotted for each cell in Fig. 9A. The data points cluster along the diagonal of slope of 1, indicating that the OI did not change during inactivation. Note that cells with a GABA effect (squares) and with no GABA effect (circles) on the preferred orientation are distributed in a similar way.

Alitto & Usrey (2004) showed that different methods of estimating the tuning width of an orientation curve could give different results (circular variance vs. half-width in their case). To verify that the OI used here was reliable, we also analysed the tuning width with the classic metrics of half-width at half-height (HWHH) (Gaussian fit, see Materials and methods) at the single-cell level. The HWHH for GABA was plotted against the HWHH for control (Fig. 9B). As expected, this analysis did not reveal changes in the tuning width, as

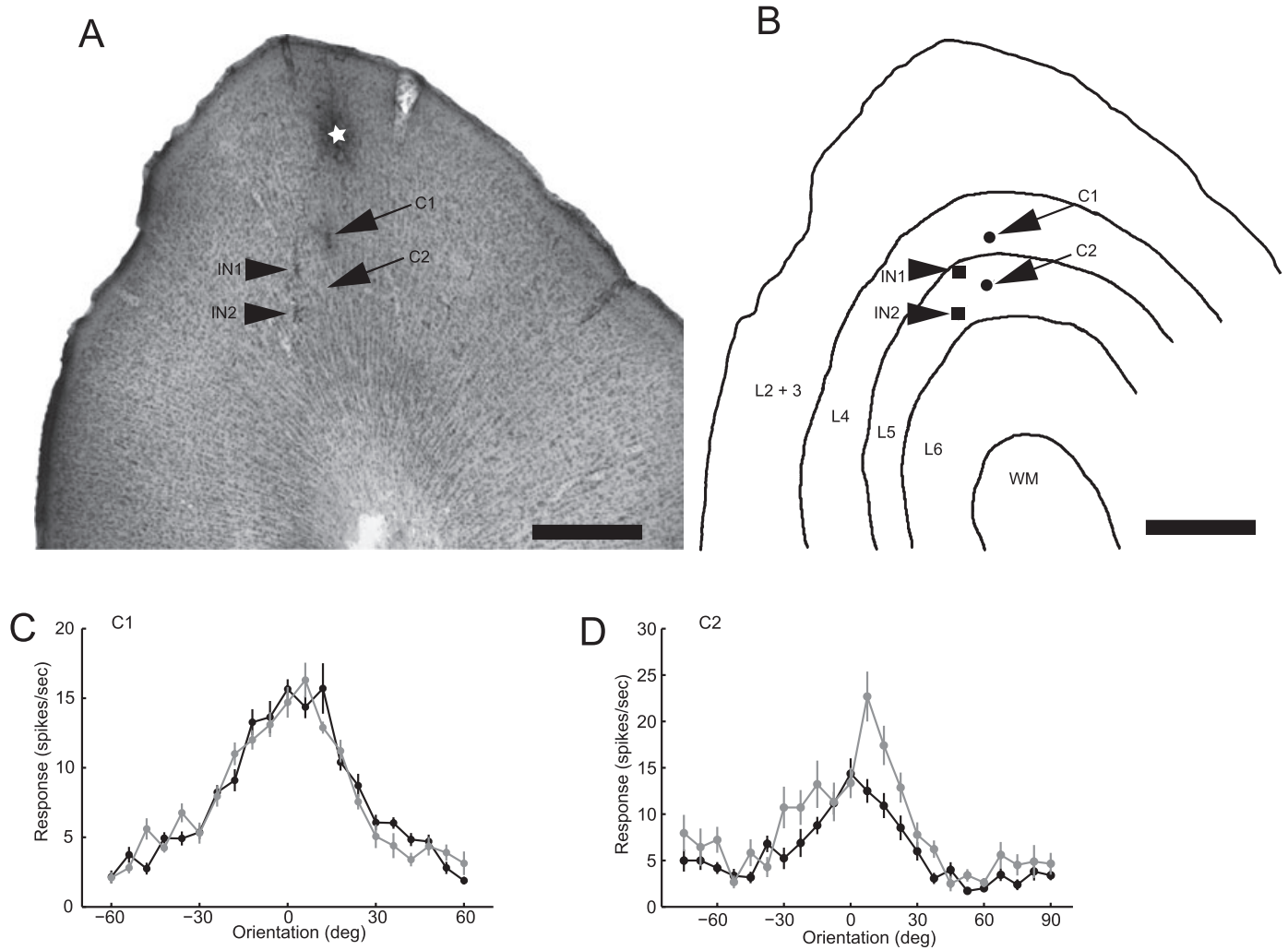


FIG. 5. Example of a penetration. (A) Coronal section through a recording and inactivation site. C1 denotes a recording site for which inactivation was performed at location IN1. C2 denotes a recording site for which inactivation was performed at location IN2. The white star shows an injection of biocytin in layer 3 from the same penetration. (B) Drawing of the section shown in A. The layer boundaries, the recording (arrows) and the injection sites (arrowheads) are shown as in A. WM, white matter. Scale bar for A and B is 500  $\mu$ m. (C) Orientation tuning curve for the recording/inactivation pair C1/IN1. (D) Orientation tuning curves for the recording/inactivation pair C2/IN2. Note that this cell is the same as in Fig. 3A. In C and D, black is control, and grey is  $\gamma$ -aminobutyric acid.

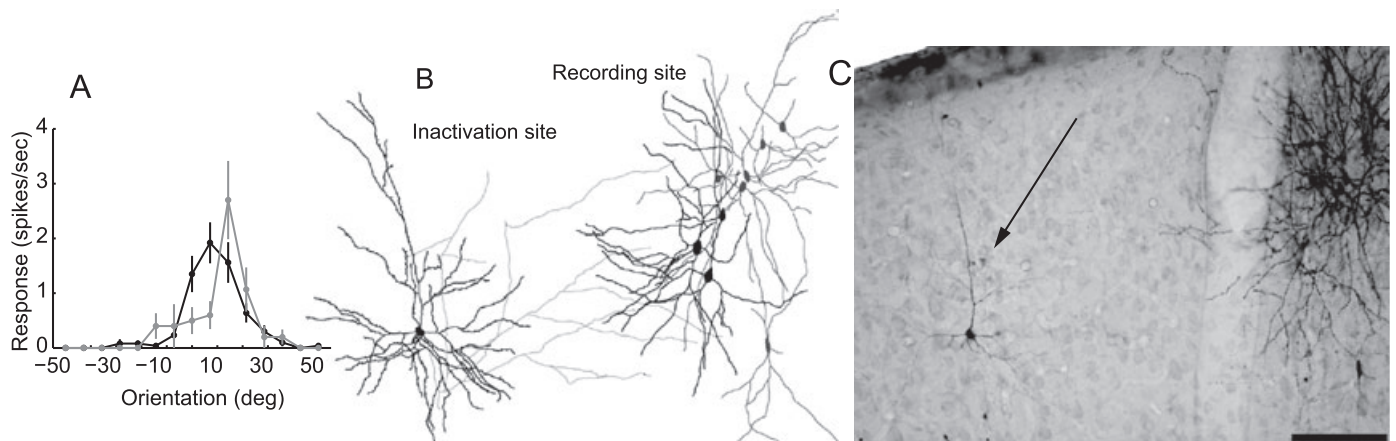


FIG. 6. Example of  $\gamma$ -aminobutyric acid (GABA) effect on a layer 2/3 cell. The inactivation was in layer 2/3. (A) Orientation tuning curves measured at the recording site (black, control; grey, GABA). (B) Partial reconstructions of the recording and inactivation sites from C. Note the axons projecting from the inactivation site to the recording site. (C) Coronal section showing the recording site on the right where biocytin was injected. A cell in the vicinity of the inactivation location (arrow) was stained retrogradely via its axon from the recording site. Scale bar is 100  $\mu$ m.

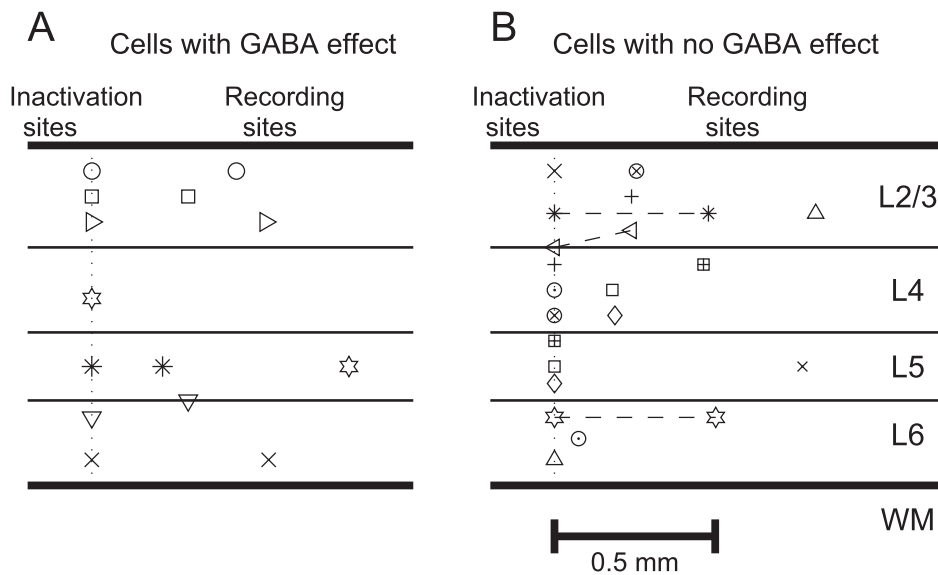


FIG. 7. Horizontal distance between inactivation and recording sites for cases where both the recording and the inactivation site could be identified histologically. (A) Cells with a significant  $\gamma$ -aminobutyric acid (GABA) effect ( $n = 7$ ). (B) Cells with no GABA effect ( $n = 11$ ). Each pair of symbols represents a pair of inactivation/recording sites. The inactivation sites have been vertically aligned for the purposes of illustration (dotted vertical line). Each recording site has then been plotted at its corresponding horizontal distance and in its corresponding layer. The vertical position within the layer is irrelevant except when the symbol lies on the line (layer border). The cortical layers are given on the right of B (WM, white matter). Layers and scale bar apply to both panels. The mean horizontal distance between recording and inactivation sites was  $451 \pm 75 \mu\text{m}$  in A and  $383 \pm 73 \mu\text{m}$  in B. Note that we found only two pairs with no GABA effect when recording and inactivating in the same layer, and one pair with inactivation on the layer border (linked with dashed lines in B). In contrast, the majority of pairs with a GABA effect were located within the same layer (A).

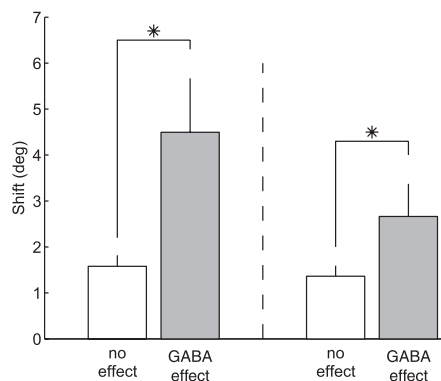


FIG. 8. Shift of the preferred orientation of the population of cells showing a significant  $\gamma$ -aminobutyric acid (GABA) effect (grey bars) and cells showing no effect (white bars). Left, comparison using a Gaussian fit. Right, comparison using a vector averaging method. In both cases, the shift of the GABA effect group is significantly larger than that of the non-GABA effect group, as indicated by the star (see text for details).

the data cluster around the diagonal. The black square in Fig. 9B corresponds to the cell presented in Fig. 4C. Obviously, a Gaussian equation does not always provide a good fit to the orientation tuning curves, as is the case in this cell, which explains the apparent increase in tuning width during GABA inactivation. However, from the analysis of the tuning width using two different methods, we can conclude that the inactivation did not produce changes in the tuning width, but only in the amplitudes of response around the peak (e.g. Fig. 4C).

For all cells, we then analysed amplitude changes by looking at the response around the peak of the tuning curve. The peak response was averaged with its two neighbouring points. We observed no systematic

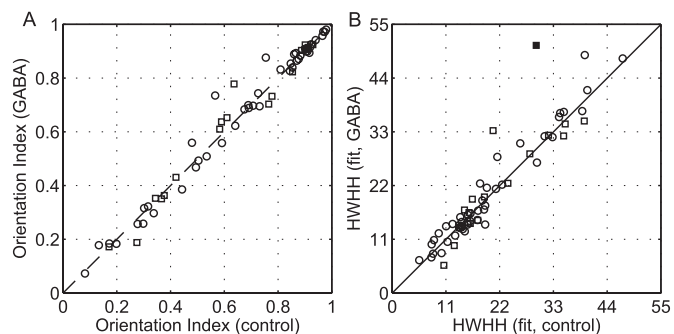


FIG. 9. Orientation index and half-width at half-height (HWHH). (A) Orientation index calculated from the mean response. The orientation indices for the control tuning curves are plotted on the  $x$ -axis, and the indices for the corresponding  $\gamma$ -aminobutyric acid (GABA) tuning curve are plotted on the  $y$ -axis. Circles represent cells with no significant GABA effect, and squares represent cells with a GABA effect on preferred orientation. The diagonal has a slope of 1. Note the absence of tuning broadening, even for cells with a significant GABA effect (squares). (B) HWHH measured on Gaussian fit for GABA vs. control recordings (axis units in degrees). The black square in B corresponds to the cell presented in Fig. 4C (see text for details). Cells with (squares) and without (circles) GABA effects on preferred orientation distribute close to the diagonal of slope 1 in both panels.

changes in response amplitude during GABA iontophoresis. Only 2/18 cells with GABA effects showed changes in amplitude (one significant increase, one significant decrease; two-sample  $t$ -test, two-tailed,  $P < 0.05$ ). For all other cells, the changes were not significant, because they were balanced: an increase in response on one side of the maximum was often accompanied by an equivalent decrease in response on the other side of the peak, so there was no net change in amplitude (e.g. Figs 4 and 6).

### Functional relationship between recording and inactivation locations

As the responses at the inactivated sites were also recorded, it was possible to measure the preferred orientation of the inactivated cells that functionally influenced the recorded cell. The preferred orientation of cells at the inactivated site could be determined in 14 cases where the recorded cell was influenced by the GABA inactivation. In Fig. 10, the difference in orientation between the recorded and inactivation sites is plotted against the peak shift of the preferred orientation. A repulsive shift (plotted as a positive value) occurred when the orientation tuning curve of the recorded cell shifted away from the preferred orientation at the inactivation site. Conversely an attractive shift (plotted as a negative value) occurred when the tuning curve shifted towards the preferred orientation recorded at the inactivation location. Three cells showed a repulsive shift, whereas 11 cells had an attractive shift. The median peak shift was  $7.5^\circ$  (see inset histograms). Four cells that had a GABA effect, but for which no orientation data at the inactivated site could be obtained, are plotted above the scatter plot (black squares). This representation shows that the shift magnitude was similar for those cells ( $x$ -axis of the scatter plot applies there as well). The average difference in preferred orientation between recorded and inactivation sites was  $29.6^\circ \pm 16.2^\circ$  (mean  $\pm$  SD) for cells with a significant GABA effect ( $n = 14$ , absolute values of  $y$ -axis from Fig. 10), whereas it was  $41.2^\circ \pm 28.7^\circ$  for 20 pairs with no GABA effect for which the preferred orientation could be measured at the inactivation sites. Nevertheless, this difference failed to reach significance (two-sample  $t$ -test, two-tailed,  $t_{32} = 1.36$ ,  $P = 0.18$ ).

### Discussion

The results show that inactivation of a small portion of the lateral input to a cell can change its preferred orientation, but does not change the cell's tuning width. GABA was used here, because, unlike local anaesthetics such as lidocaine, it only inactivates cells and not *en passant* fibres (Hupé *et al.*, 1999). Moreover, because GABA is a neurotransmitter, the GABA uptake mechanisms ensure that the recovery after GABA iontophoresis occurs within seconds, thus

permitting interleaved trial protocols (see Fig. 1), which are not possible with GABA receptor agonists such as muscimol, where recovery can take 4 h or more (Grieve & Sillito, 1991).

### Technical considerations

We used an interleaved protocol to avoid the influence of non-specific changes in excitability that occur over time even in the most physiologically stable preparations. With this protocol, changes in a cell's excitability over the time course of the recording, for example, would be averaged out. This is not the case when block designs are used and the control, GABA and recovery epochs follow sequentially (Crook *et al.*, 1991; Crook & Eysel, 1992). In the interleaved protocol, complete recovery was ensured by excluding 60–90 s of recording after the termination of each GABA iontophoresis period.

Direct effects of GABA by diffusion from the inactivation site to the recording site can be excluded, as we showed that spontaneous activity did not decrease in the cells that had a GABA effect, even if the recorded cell was as close as  $220 \mu\text{m}$  to the inactivation pipette. In this particular cell (Fig. 3A), the spontaneous activity did not decrease during GABA iontophoresis; on the contrary, the response close to the optimal orientation increased. This is consistent with a disinhibitory, not an inhibitory, effect. Several studies have shown that GABA would not diffuse more than  $200 \mu\text{m}$  under the ejection currents and durations used here (Herz *et al.*, 1969; Crook *et al.*, 1998; Hupé *et al.*, 1999; Martinez-Conde *et al.*, 1999).

### Comparison with other studies

Our results are partly in agreement with those of previous studies using lateral inactivation methods (Crook *et al.*, 1991; Crook & Eysel, 1992). Crook *et al.* (1991) also reported a shift in preferred orientation in some 25% of the cells, but this was always accompanied by a broadening of orientation tuning. The loss of orientation selectivity that they found was thought to be due to a loss of lateral inhibition from large basket cells (Crook *et al.*, 1998) [see also Crook *et al.*

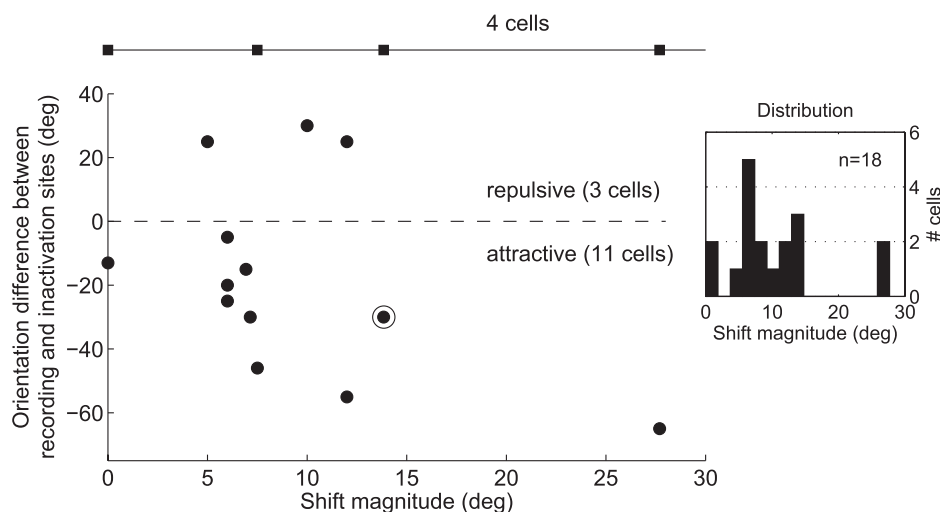


FIG. 10. Scatter plot of the preferred orientation difference between the recording and the inactivation sites ( $y$ -axis) as a function of the preferred orientation shift [ $x$ -axis, difference between the peak of the control and the  $\gamma$ -aminobutyric acid (GABA) tuning curve]. Each dot corresponds to one cell ( $n = 14$ ) that showed a GABA effect and for which the preferred orientation at the inactivation site could be determined. The dot within a circle represents two cells that overlap. Positive orientation differences represent a repulsive shift, whereas negative values represent an attractive shift (see text). The top line shows four cells (squares) for which the preferred orientation at the inactivation site could not be determined. The  $x$ -axis of the lower panel applies to the top line graph. Note that the peak shifts for those cells are similar to those for other cells. Two cells with peaks at identical positions but with functional shifts are included (dot and square on the  $y$ -axis; see Materials and methods for details). The inset histograms show the distribution of shift magnitudes. The median is  $7.5^\circ$ .

(2002) for a review of their results]. In this study, we did not observe a significant increase in tuning width. The discrepancy can have different origins. First, Crook & Eysel (1992) reported that the GABA effect peaked 10–15 min after iontophoresis onset, whereas in the present experiments the inactivation time never exceeded 3 min. Second, in some cases they used multiple inactivation sites, whereas only one inactivation site was used here. Multiple inactivation sites are likely to have a stronger effect on the recorded cell. Third, because the axons of superficial layer pyramidal cells form a patchy architecture (referred to as a ‘Daisy’) (Douglas & Martin, 2004), with a like-to-like connectivity pattern, we targeted similar orientation columns for recording and inactivation using optical imaging maps (see Materials and methods). By contrast, Crook *et al.* found that a broadening occurred when the inactivation and recording sites had dissimilar orientation preferences; hence their interpretation that the effect was caused by a reduction in cross-orientation inhibition (Crook & Eysel, 1992).

In subsequent experiments, Crook *et al.* (1997) found a change in orientation width in only 5% of the cells when the preferred orientation at the inactivation site and at the recorded site was similar (within  $22.5^\circ$ ). In those cases of remote inactivation, the main effect was to reduce or increase the directionality of 65% of the cells. We did not observe such an effect, although, in the interest of reducing the total recording time, direction selectivity was not tested systematically. The small shifts in orientation tuning that we observed would not have been detected by Crook *et al.* (1997), because they used much larger stimulus increments ( $22.5^\circ$ ) than the  $4\text{--}14^\circ$  increments that we used. Finally, we stimulated with drifting gratings, whereas Crook *et al.* used moving and flashed bars.

Previous investigations with bicuculline (a GABA<sub>A</sub> receptor antagonist) reported that blocking the GABA<sub>A</sub> receptor broadened the tuning curves. The effects of bicuculline on orientation tuning were more marked in cat area 17 complex cells following transient than following sustained stimuli (Pfleger & Bonds, 1995), and temporal frequency tuning broadened more than orientation or spatial frequency tuning in cat area 18 cells (Vidyasagar & Heide, 1986). This suggests either that different stimuli recruit different amounts of inhibition (probably through the activation of different circuits), or that the effect also depends on the area of cortex being tested, as recently shown by Jirmann *et al.* (2009).

#### Cortical circuit involved

The vast majority of synapses in the cat’s V1 are provided by other excitatory cells of the cortex. The thalamocortical synapses represent only about 5% of the excitatory synapses even in layer 4, the main termination layer of the thalamic afferents (Peters & Payne, 1993; Ahmed *et al.*, 1994; Binzegger *et al.*, 2004). The traditional view of cortical processing is that it occurs through hierarchical, feedforward circuits, which are sequenced through the laminar organization of the cortex (Hubel & Wiesel, 1962; Felleman & Van Essen, 1991). The role of the lateral connections, which constitute a major component of local circuit synapses (Binzegger *et al.*, 2004), is not well understood. One view is that lateral inhibition is critical for cortical functions, such as orientation selectivity. This relationship between orientation selectivity and inhibition has a long and controversial history (Martin, 1988). Orientation tuning was studied in pharmacological experiments with bicuculline to block inhibition, and the authors concluded that GABAergic inhibition is essential for orientation selectivity (Pettigrew & Daniels, 1973; Daniels & Pettigrew, 1975; Sillito, 1975, 1979; Tsumoto *et al.*, 1979; Sillito *et al.*, 1980; Nelson, 1991; Sato *et al.*, 1996; Eysel *et al.*, 1998). However, because inhibition is blocked,

excitation is greater, so the results have several possible interpretations. These authors assume that the inhibitory cells, which sharpen the tuning of other cells, are themselves tuned for orientation [see Vidyasagar *et al.* (1996) for discussion] and thus provide cross-orientation inhibition (Morrone *et al.*, 1982). Non-oriented inhibitory input has been proposed as well (Hirsch *et al.*, 2003; Nowak *et al.*, 2008) [but see Cardin *et al.* (2007)].

When inhibition was blocked intracellularly, the preferred orientation was preserved (Nelson *et al.*, 1994), although directionality was impaired in some cases. The interpretation was that the cortical cells receive their excitatory inputs from their immediate neighbours, who retain their orientation selectivity. Although the arrangement of thalamic inputs may provide the initial seed for orientation selectivity (Hubel & Wiesel, 1962), it is clear that this feedforward circuit is insufficient to account for the results of lateral inactivation, which indicate that changes in the local circuit activity modify the orientation tuning and the directionality of cortical neurons (present study; Crook *et al.*, 1991; Crook & Eysel, 1992).

#### What could orientation shifts be good for?

Repulsive shifts of orientation tuning were reported in experiments using adaptation to manipulate the cortical circuit (Müller *et al.*, 1999; Dragoi *et al.*, 2000, 2001; Felsen *et al.*, 2002). In these experiments, the cell’s preferred orientation shifted away (a ‘repulsive’ shift) from the adapting stimulus. The change in orientation sensitivity is thought to involve a local change in gain (Dragoi *et al.*, 2000), a role for which the lateral clusters of excitatory terminals of the Daisy are well-suited. A shift of the orientation tuning curve was also reported in stimulus

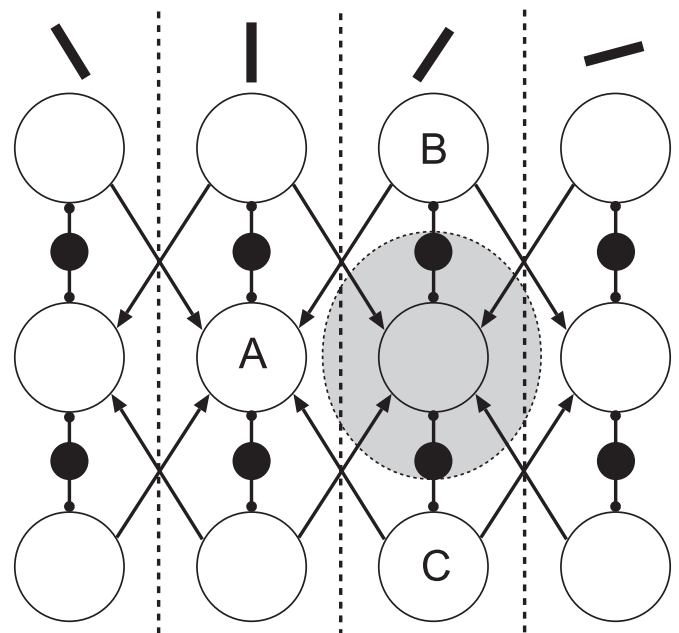


FIG. 11. Schematic circuit (top view) to explain the attractive shift in orientation tuning. The orientation domains are separated by dashed lines, and the preferred orientation is shown on the top as a thick line. Only dominant connections are shown (see text for details). Excitatory cells (white circles) have longer axons than inhibitory cells (black, filled circles). The greyed area represents the inactivated region. Cells B and C receive less short-range inhibition, due to inactivation. On the other hand, they still contact cell A. This results in a shift of the preferred orientation of cell A towards the preferred orientation of cells at the inactivated location.

timing-dependent experiments (Yao & Dan, 2001). In this case, the shift direction (away or towards the test stimulus) depends on the relative timing between the two stimuli. In area MT (middle temporal visual area or area V5), in contrast to V1, in the macaque, adaptation to the stimulus direction produced an attractive shift in direction preference (Kohn & Movshon, 2004).

Teich & Qian (2003) built a recurrent network composed of cells with a preferred orientation, as in V1, and showed that the cells can shift their preferred orientation by modifying the lateral connections. In most models of orientation selectivity, the circuit is implemented with a 'Mexican hat' configuration, in which the lateral extent of inhibition is greater than for excitation, so that the surround inhibition provides the means by which a cell's selectivity is sharpened. However, the reverse pattern is actually the case: the inhibitory cells form the majority of their synapses locally within 500  $\mu\text{m}$  (Buzás *et al.*, 2001), and the inhibitory axons extend less than the excitatory axons (Douglas & Martin, 1998).

Our results show that a small region of inactivation (about 200  $\mu\text{m}$  in diameter) has a detectable effect on the response of a neuron. How this is mediated by the underlying circuits is still a matter of conjecture. The work of Buzás *et al.* (2001, 2006) and Binzegger *et al.* (2007) indicates that many quantitative details of the lateral connections are still unknown, but we offer a schematic circuit that may explain qualitatively the attractive shift that we observed (Fig. 11).

The circuit is presented as a top view of the cortex with four preferred orientation columns. Only the dominant connections (estimated by number of synapses) are shown (for example, 'long-range' connections of inhibitory neurons are omitted because they constitute only a small proportion of all synapses formed by these cells). Instead of the 'Mexican hat' connection profile, the excitatory cells here have longer lateral connections than inhibitory cells, as is seen *in vivo*. Thus, cells are connected to neighbouring columns via excitatory connections, whereas inhibition is local. Note, however, that the constraint of the Daisy architecture, that the excitatory connections avoid orthogonal orientation columns, is preserved. During a local inactivation, the longer-range excitatory connections between columns remain functional, while the shorter-range inhibitory connections are silenced. This is shown in Fig. 11, where cells B and C, located outside of the inactivated region, receive less inhibition than under control conditions, but still contribute to exciting cell A. This results in a shift of the preferred orientation of cell A towards the preferred orientation of cells C and B. Such a circuit might be used by the cortex to bias the preferred orientation of cells, and thus provide a means of modulating the cell's response, as is required for learning or adaptation [see, for example, Dragoi *et al.* (2000) and Schoups *et al.* (2001)].

## Acknowledgements

We thank Anita Schmid, Pamela Baker, Elisha Rüscher, Laureston Kellaway, Nuno da Costa and John Anderson for support in the experiments. This work was supported by EU Daisy grant number FP6-2005-015803.

## Abbreviations

GABA,  $\gamma$ -aminobutyric acid; HWHH, half-width at half-height; OI, orientation index; V1, primary visual cortex.

## References

Ahmed, B., Anderson, J.C., Douglas, R.J. & Martin, K.A. (1994) Polyneuronal innervation of spiny stellate neurons in cat visual cortex. *J. Comp. Neurol.*, **341**, 39–49.

- Alitto, H.J. & Usrey, W.M. (2004) Influence of contrast on orientation and temporal tuning frequency in ferret primary visual cortex. *J. Neurophysiol.*, **91**, 2797–2808.
- Binzegger, T., Douglas, R.J. & Martin, K.A.C. (2004) A quantitative map of the circuit of cat primary visual cortex. *J. Neurosci.*, **24**, 8441–8453.
- Binzegger, T., Douglas, R.J. & Martin, K.A.C. (2007) Stereotypical bouton clustering of individual neurons in cat primary visual cortex. *J. Neurosci.*, **27**, 12242–12254.
- Buzás, P., Eysel, U.T., Adorjan, P. & Kisvárdy, Z.F. (2001) Axonal topography of cortical basket cells in relation to orientation, direction, and ocular dominance maps. *J. Comp. Neurol.*, **437**, 259–285.
- Buzás, P., Kovács, K., Ferecskó, A.S., Budd, J.M., Eysel, U.T. & Kisvárdy, Z.F. (2006) Model-based analysis of excitatory lateral connections in the visual cortex. *J. Comp. Neurol.*, **499**, 861–881.
- Callaway, E.M. & Katz, L.C. (1990) Emergence and refinement of clustered horizontal connections in cat striate cortex. *J. Neurosci.*, **10**, 1134–1153.
- Callaway, E.M. & Katz, L.C. (1991) Effects of binocular deprivation on the development of clustered horizontal connections in cat striate cortex. *Proc. Natl Acad. Sci. USA*, **88**, 745–749.
- Cardin, J.A., Palmer, L.A. & Contreras, D. (2007) Stimulus feature selectivity in excitatory and inhibitory neurons in primary visual cortex. *J. Neurosci.*, **26**, 10333–10344.
- Crook, J.M. & Eysel, U.T. (1992) GABA-induced inactivation of functionally characterized sites in cat visual cortex (area 18): effects on orientation tuning. *J. Neurosci.*, **12**, 1816–1825.
- Crook, J.M., Eysel, U.T. & Machemer, H.F. (1991) Influence of GABA-induced remote inactivation on the orientation tuning of cells in area 18 of feline visual cortex: a comparison with area 17. *Neuroscience*, **40**, 1–12.
- Crook, J.M., Kisvárdy, Z.F. & Eysel, U.T. (1997) GABA-induced inactivation of functionally characterized sites in cat striate cortex: effects on orientation tuning and direction selectivity. *Vis. Neurosci.*, **14**, 141–158.
- Crook, J.M., Kisvárdy, Z.F. & Eysel, U.T. (1998) Evidence for a contribution of lateral inhibition to orientation tuning and direction selectivity in cat visual cortex: reversible inactivation of functionally characterized sites combined with neuroanatomical tracing techniques. *Eur. J. Neurosci.*, **10**, 2056–2075.
- Crook, J.M., Kisvárdy, Z.F. & Eysel, U.T. (2002) Intracortical mechanisms underlying orientation and direction selectivity studied with GABA-inactivation technique. In Lomber, S.G. & Galuske, R.A. (Eds), *Virtual Lesions: Examining Cortical Function with Reversible Deactivation*. Oxford University Press, New York, pp. 3–40.
- Daniels, J.D. & Pettigrew, J.D. (1975) A study of inhibitory antagonism in cat visual cortex. *Brain Res.*, **93**, 41–62.
- Douglas, R.J. & Martin, K.A. (1998) Neocortex. In Shepherd, G.M. (Ed.), *The Synaptic Organization of the Brain*. Oxford University Press, Oxford, pp. 459–509.
- Douglas, R.J. & Martin, K.A. (2004) Neuronal circuits of the neocortex. *Annu. Rev. Neurosci.*, **27**, 419–451.
- Dragoi, V., Sharma, J. & Sur, M. (2000) Adaptation-induced plasticity of orientation tuning in adult visual cortex. *Neuron*, **28**, 287–298.
- Dragoi, V., Rivadulla, C. & Sur, M. (2001) Foci of orientation plasticity in visual cortex. *Nature*, **411**, 80–86.
- Eysel, U.T., Crook, J.M. & Machemer, H.F. (1990) GABA-induced remote inactivation reveals cross-orientation inhibition in the cat striate cortex. *Exp. Brain Res.*, **80**, 626–630.
- Eysel, U.T., Shevelev, I.A., Lazareva, N.A. & Sharaev, G.A. (1998) Orientation tuning and receptive field structure in cat striate neurons during local blockade of intracortical inhibition. *Neuroscience*, **84**, 25–36.
- Felleman, D.J. & Van Essen, D.C. (1991) Distributed hierarchical processing in the primate cerebral cortex. *Cereb. Cortex*, **1**, 1–47.
- Felsen, G., Shen, Y.S., Yao, H., Spor, G., Li, C. & Dan, Y. (2002) Dynamic modification of cortical orientation tuning mediated by recurrent connections. *Neuron*, **36**, 945–954.
- Ferster, D. & Miller, K.D. (2000) Neural mechanisms of orientation selectivity in the visual cortex. *Annu. Rev. Neurosci.*, **23**, 441–471.
- Gilbert, C.D. & Wiesel, T. (1989) Columnar specificity of intrinsic horizontal and corticocortical connections in cat visual cortex. *J. Neurosci.*, **9**, 2432–2442.
- Girardin, C.C., Kiper, D.C. & Martin, K.A. (2002) The effect of moving textures on the responses of cells in the cat's dorsal lateral geniculate nucleus. *Eur. J. Neurosci.*, **16**, 2149–2156.
- Grieve, K.L. & Sillito, A.M. (1991) A re-appraisal of the role of layer VI of the visual cortex in the generation of cortical end inhibition. *Exp. Brain Res.*, **87**, 521–529.

- Herz, A., Zieglansberger, W. & Farber, G. (1969) Microelectrophoretic studies concerning the spread of glutamic acid and GABA in brain tissue. *Exp. Brain Res.*, **9**, 221–235.
- Hirsch, J.A., Martínez, L.M., Pillai, C., Alonso, J.M., Wang, Q. & Sommer, F.T. (2003) Functionally distinct inhibitory neurons at the first stage of visual cortical processing. *Nat. Neurosci.*, **6**, 1300–1308.
- Hubel, D. & Wiesel, T. (1962) Receptive fields, binocular interaction and functional architecture in the cat's visual cortex. *J. Physiol.*, **160**, 106–154.
- Hupé, J.M., Chouvet, G. & Bullier, J. (1999) Spatial and temporal parameters of cortical inactivation by GABA. *J. Neurosci. Methods*, **86**, 129–143.
- Jirjann, U.K., Pernberg, J. & Eysel, U.T. (2009) Region-specificity of GABA<sub>A</sub> receptor mediated effects on orientation and direction selectivity in cat visual cortical area 18. *Exp. Brain Res.*, **192**, 369–378.
- Kisvárdy, Z.F. & Eysel, U.T. (1992) Cellular organization of reciprocal patchy networks in layer III of cat visual cortex (area 17). *Neuroscience*, **46**, 275–286.
- Kisvárdy, Z.F., Martin, K.A., Whitteridge, D. & Somogyi, P. (1985) Synaptic connections of intracellularly filled clutch cells: a type of small basket cell in the visual cortex of the cat. *J. Comp. Neurol.*, **241**, 111–137.
- Kisvárdy, Z.F., Tóth, E., Rausch, M. & Eysel, U.T. (1997) Orientation-specific relationship between populations of excitatory and inhibitory lateral connections in the visual cortex of the cat. *Cereb. Cortex*, **7**, 605–618.
- Kohn, A. & Movshon, J.A. (2004) Adaptation changes the direction tuning of macaque MT neurons. *Nat. Neurosci.*, **7**, 764–772.
- LeVay, S. (1986) Synaptic organization of claustral and geniculate afferents to the visual cortex of the cat. *J. Neurosci.*, **6**, 3564–3575.
- Lübke, J. & Albus, K. (1992) Lack of exuberance in clustered intrinsic connections in the striate cortex of one-month-old kitten. *Eur. J. Neurosci.*, **4**, 189–192.
- Luhmann, H.J., Singer, W. & Martínez-Millán, L. (1990) Horizontal interactions in cat striate cortex: I. Anatomical substrate and postnatal development. *Eur. J. Neurosci.*, **2**, 344–357.
- Mariño, J., Schummers, J., Lyon, D.C., Schwabe, L., Beck, O., Wiesing, P., Obermayer, K. & Sur, M. (2005) Invariant computations in local cortical networks with balanced excitation and inhibition. *Nat. Neurosci.*, **8**, 194–201.
- Martin, K.A. (1988) The Wellcome Prize lecture. From single cells to simple circuits in the cerebral cortex. *Q. J. Exp. Physiol.*, **73**, 637–702.
- Martin, K.A. (2002) Microcircuits in visual cortex. *Curr. Opin. Neurobiol.*, **12**, 418–425.
- Martin, K.A. & Whitteridge, D. (1984) Form, function and intracortical projections of spiny neurones in the striate visual cortex of the cat. *J. Physiol.*, **353**, 463–504.
- Martin, K.A., Somogyi, P. & Whitteridge, D. (1983) Physiological and morphological properties of identified basket cells in the cat's visual cortex. *Exp. Brain Res.*, **50**, 193–200.
- Martínez-Conde, S., Cudeiro, J., Grieve, K.L., Rodríguez, R., Rivadulla, C. & Acuna, C. (1999) Effects of feedback projections from area 18 layers 2/3 to area 17 layers 2/3 in the cat visual cortex. *J. Neurophysiol.*, **82**, 2667–2675.
- Morrone, M.C., Burr, D.C. & Maffei, L. (1982) Functional implications of cross-orientation inhibition of cortical visual cells. I. Neurophysiological evidence. *Proc. R. Soc. Lond. B Biol. Sci.*, **216**, 335–354.
- Müller, J.R., Metha, A.B., Krauskopf, J. & Lennie, P. (1999) Rapid adaptation in visual cortex to the structure of images. *Science*, **285**, 1405–1408.
- Nelson, S.B. (1991) Temporal interactions in the cat visual system. III. Pharmacological studies of cortical suppression suggest a presynaptic mechanism. *J. Neurosci.*, **11**, 169–380.
- Nelson, S., Toth, L., Sheth, B. & Sur, M. (1994) Orientation selectivity of cortical neurons during intracellular blockade of inhibition. *Science*, **265**, 774–777.
- Nowak, L.G., Sanchez-Vives, M.V. & McCormick, D.A. (2008) Lack of orientation and direction selectivity in a subgroup of fast-spiking inhibitory interneurons: cellular and synaptic mechanisms and comparison with other electrophysiological cell types. *Cereb. Cortex*, **18**, 1058–1078.
- Ohzawa, I., Sclar, G. & Freeman, R.D. (1985) Contrast gain control in the cat's visual system. *J. Neurophysiol.*, **54**, 651–667.
- Peters, A. & Payne, B.R. (1993) Numerical relationships between geniculocortical afferents and pyramidal cell modules in cat primary visual cortex. *Cereb. Cortex*, **3**, 69–78.
- Pettigrew, J.D. & Daniels, J.D. (1973) Gamma-aminobutyric acid antagonism in visual cortex: different effects on simple, complex, and hypercomplex neurons. *Science*, **182**, 81–83.
- Pfleger, B. & Bonds, A.B. (1995) Dynamic differentiation of GABA<sub>A</sub>-sensitive influences on orientation selectivity of complex cells in the cat striate cortex. *Exp. Brain Res.*, **104**, 81–88.
- Reid, R.C. & Alonso, J.-M. (1995) Specificity of monosynaptic connections from thalamus to visual cortex. *Nature*, **378**, 281–284.
- Sato, H., Katsuyama, N., Tamura, H., Hata, Y. & Tsumoto, T. (1996) Mechanisms underlying orientation selectivity of neurons in the primary visual cortex of the macaque. *J. Physiol.*, **494**, 757–771.
- Schmidt, K.E., Goebel, R., Löwel, S. & Singer, W. (1997) The perceptual grouping criterion of colinearity is reflected by anisotropies of connections in the primary visual cortex. *Eur. J. Neurosci.*, **9**, 1083–1089.
- Schoups, A., Vogels, R., Qian, N. & Orban, G. (2001) Practising orientation identification improves orientation coding in V1 neurons. *Nature*, **412**, 543–553.
- Sillito, A.M. (1975) The contribution of inhibitory mechanisms to the receptive field properties of neurones in the striate cortex of the cat. *J. Physiol.*, **250**, 305–329.
- Sillito, A.M. (1979) Inhibitory mechanisms influencing complex cell orientation selectivity and their modification at high resting discharge levels. *J. Physiol.*, **289**, 33–53.
- Sillito, A.M., Kemp, J.A., Milson, J.A. & Berardi, N. (1980) A re-evaluation of the mechanisms underlying simple cell orientation selectivity. *Brain Res.*, **194**, 517–520.
- Swindale, N.V. (1998) Orientation tuning curves: empirical description and estimation of parameters. *Biol. Cybern.*, **78**, 45–56.
- Teich, A.F. & Qian, N. (2003) Learning and adaptation in a recurrent model of V1 orientation selectivity. *J. Neurophysiol.*, **89**, 2086–2100.
- Tsumoto, T., Eckart, W. & Creutzfeldt, O.D. (1979) Modification of orientation sensitivity of cat visual cortex neurons by removal of GABA-mediated inhibition. *Exp. Brain Res.*, **34**, 351–363.
- Vidyasagar, T.R. & Heide, W. (1986) The role of GABAergic inhibition in the response properties of neurones in cat visual area 18. *Neuroscience*, **17**, 49–55.
- Vidyasagar, T.R., Pei, X. & Volgushev, M. (1996) Multiple mechanisms underlying the orientation selectivity of visual cortical neurones. *Trends Neurosci.*, **19**, 272–277.
- Winfield, D.A. & Powell, T.P. (1983) Laminar cell counts and geniculocortical boutons in area 17 of cat and monkey. *Brain Res.*, **277**, 223–229.
- Yao, H. & Dan, Y. (2001) Stimulus timing-dependent plasticity in cortical processing of orientation. *Neuron*, **32**, 315–323.
- Yousef, T., Bonhoeffer, T., Kim, D.S., Eysel, U.T., Tóth, E. & Kisvárdy, Z.F. (1999) Orientation topography of layer 4 lateral networks revealed by optical imaging in cat visual cortex (area 18). *Eur. J. Neurosci.*, **11**, 4291–4308.
- Yousef, T., Tóth, E., Rausch, M., Eysel, U.T. & Kisvárdy, Z.F. (2001) Topography of orientation centre connections in the primary visual cortex of the cat. *Neuroreport*, **12**, 1693–1699.